ARTICLE
Journal of Cellular Biochemistry 106:327–336 (2009)

Journal of Cellular Biochemistry

Defects in Intracellular Trafficking and Endocytic/Vacuolar Acidification Determine the Efficiency of Endocytotic DNA Uptake in Yeast

Sean-Patrick Riechers, Ulf Stahl, and Christine Lang*

Department of Microbiology and Genetics, Institute for Biotechnology, Technische Universität Berlin, Gustav-Meyer-Allee 25, D-13355 Berlin, Germany

ABSTRACT

The yeast *Saccharomyces cerevisiae* is a standard model system to study endocytosis. Here we describe the examination of a representative subset of deletion mutants to identify and locate steps in endocytic transport, endosomal/lysosomal acidification and in intracellular transport of hydrolases in non-viral transfection processes. When transport in late endocytosis is inhibited, transfection efficiency is significantly enhanced. Similarly, transfection efficiency is enhanced when the pH-value of the endosomal/vacuolar system is modified. Transfection efficiency is furthermore elevated when the Na^+/K^+ transport in the endosomal system is disturbed. Finally, we observe enhanced transfection efficiency in mutants disturbed in the CVT/autophagy pathway and in hydrolase transport to the vacuole. In summary, non-viral transfection efficiency can be significantly increased by either (i) inhibiting the transport of endocytosed material before it enters the vacuole, or (ii) inducing a non-natural pH-value of the endosomal/vacuolar system, or (iii) slowing down degradative processes by inhibiting vacuolar hydrolases or the transport between Golgi and late endosome/vacuole. J. Cell. Biochem. 106: 327–336, 2009.

KEY WORDS: ENDOCYTOSIS; LYSOSOME; NON-VIRAL TRANSFECTION; VACUOLE; YEAST

The yeast *Saccharomyces cerevisiae* is a standard model for studying endocytosis [Shaw et al., 2001]. In previous studies, we were able to establish yeast as a model for endocytosis-mediated non-viral transfection [Neukamm et al., 2002, 2006]. The transfection assay is based on the uptake of the naked DNA vector by endocytosis and the subsequent liberation of the DNA from the endocytic/vacuolar system by an induced osmotic shift. When using sucrose or sorbitol in equal osmolarities, DNA uptake was shown to be indeed endocytosis dependent. Transfection is achieved in sucrose solutions only, but not in sorbitol, indicating that uptake is an active and energy-dependent process. Both LY-CH and FM4-64 staining and the low efficiency of transfection in the endocytosis deficient mutant *end3* further affirm that endocytosis is the uptake mechanism for DNA in this assay [Neukamm et al., 2002]. The findings of the yeast model could successfully be transferred to a human cancer cell line (HepG2). Transfection enhancers identified in the yeast system were confirmed in the mammalian system [Neukamm et al., 2006].

To understand in detail the transport of vector DNA after the endocytic uptake and to elucidate potential bottlenecks for non-viral transfection approaches, we used selected yeast mutants, which are deleted for genes typical for specific steps in intracellular transport. In yeast endocytosis the clathrin-dependent internalisation pathway is relevant [Baggett and Wendland, 2001]. Clathrin-dependent internalisation seems to be dependent on actin both in mammalian [Yarar et al., 2005] and yeast cells [Kaksonen et al., 2005]. After internalisation, the vesicles are uncoated by a process dependent on the auxin homologue Swa2p before they fuse to early endosomal membranes. Some proteins coming from the *trans* Golgi network (TGN) are sorted into the early endosome. Many proteins sorted via the TGN are also sorted via the next compartment, the late endosome, also known as prelysosomal or prevacuolar compartment

Grant sponsor: German Federal Ministry of Education and Research (BMBF) (RiNA GmbH and Cytonet GmbH & Co. KG).

Sean-Patrick Riechers's present address is Max-Delbrück Center for Molecular Medicine, Robert-Rössle-Straße 10, D-13125 Berlin, Germany.

*Correspondence to: Dr. Christine Lang, Department of Microbiology and Genetics, Institute for Biotechnology, Technische Universität Berlin, Gustav-Meyer-Allee 25, D-13355 Berlin, Germany.
E-mail: christine.lang@tu-berlin.de

Received 6 May 2008; Accepted 5 November 2008 • DOI 10.1002/jcb.22009 • 2008 Wiley-Liss, Inc.
Published online 29 December 2008 in Wiley InterScience (www.interscience.wiley.com).

(PVC) [Gerrard et al., 2000] or the multivesicular body (MVB). Here, proteins sorted via the CPY sorting pathway from TGN to PVC meet with endocytosed material on the way to the vacuole [Bryant et al., 1998].

In addition to the CPY sorting pathway, the ALP pathway, named for its most prominent cargo alkaline phosphatase, transports material directly to the vacuole from the TGN, bypassing the late endosome [Panek et al., 1997; Darsow et al., 2001].

Finally, proteins, parts of the nucleus and even whole organelles are transported into the vacuole via the cytosol-to-vacuole-targeting (CVT)/autophagy pathway. As an example for the CVT pathway, Atg19p functions as receptor for the vacuolar aminopeptidase (API). API is bound at Atg19p clusters and is taken up into the vacuole [Scott et al., 2001]. In addition, cells recycle mitochondria by autophagy and show piecemeal microautophagy of the nucleus (PMN), under starvation conditions [Pan et al., 2000; Roberts et al., 2003] by nucleus–vacuole junctions (NVJ).

It is still unclear which of these processes play a role in endocytosis-based DNA delivery in non-viral transfection. We analysed endocytosis mutants (*rcy1*, *vps21*, *vps45*, *vps27*, *vps4* and *vam6*), endocytic/vacuolar pH- and ion homeostasis mutants (*stv1*, *vph1*, *nhx1*, *vcx1* and *pmc1*), Golgi to endosome/vacuole transport mutants (*vps13*, *vps17* and *apl5*) and CVT/autophagy mutants (*atg19* and *vac8*) to understand their specific involvement in DNA transfection.

Some parameters influencing non-viral transfection efficiency in mammalian cells have been discussed [Akinc and Langer, 2002; Wilber et al., 2002; Howell et al., 2003], these include pH-conditions and the role of lysosomal DNases in non-viral transfection. Non-functional V-ATPase correlates with reduced endocytic transport [Klionsky et al., 1992]. Protein activities are influenced by pH-value and ionic composition of the endocytic system as described for Kex2p, whose activity is dependent on K^+-ion concentration, for example [Rockwell and Fuller, 2002].

To enhance understanding and to describe an optimised way to apply endocytosis-based transfection, we use the yeast model to identify steps affecting the efficiency of transfer of endocytosed DNA by applying a rational and integrative approach. We specifically analysed the influence of endocytic transport, endosomal/vacuolar pH-value, ionic composition of the late endosome, the influence of autophagy, and the ALP sorting pathway on non-viral transfection.

MATERIALS AND METHODS

STRAINS AND CULTURE CONDITIONS

S. cerevisiae mutants used in this study are derivatives of the EUROFAN II strain BY4741 (*MATa*, *his3Δ1*, *leu2Δ0*, *met15Δ0*, *ura3Δ0*) [Brachmann et al., 1998]. The BY4741 strain is referred to as a wild-type strain further on. The mutants were grown at 28°C in YPD (1% yeast extract, 2% peptone and 2% dextrose) with reciprocal shaking at 120 rpm. YE medium with agar (0.5% yeast extract and 2% dextrose, 1.5% agar, pH 6.3) was used for non-selective conditions in transfection experiments; selective medium used was WMIX minimal medium with agar [Neukamm et al., 2002] (2% dextrose, 1% sodium L-glutamate, 0.075 g L^{-1} meso-inositol, 0.25 g L^{-1} $MgCl_2 \cdot 6H_2O$, 0.1 g L^{-1} $CaCl_2 \cdot 2H_2O$, 0.55 g L^{-1} $MgSO_4 \cdot 7H_2O$, 20 mM potassium-phosphate buffer pH 6.5, 1.5% agar, trace elements and vitamins as described for WMVIII) supplemented with casaminoacids (1 g L^{-1}), histidine (100 mg L^{-1}), methionine (80 mg L^{-1}) and leucine (40 mg L^{-1}).

Escherichia coli SF8 (*recBC*, *lop11*, *tonA1*, *thr1*, *leuB6*, *thy1*, *lacY1*, *supE44*, *hsm*$^-$, *hsr*$^-$) was used as a host for plasmid pFL1 [Botstein et al., 1979]. pFL1 carrying the *S. cerevisiae URA3* gene as a selective marker was used in transfection experiments. The cells were grown on Luria–Bertani (LB) medium containing 100 mg L^{-1} ampicillin at 37°C with 160 rpm reciprocal shaking.

PLASMID PURIFICATION

pFL1 was purified using the Qiagen plasmid purification kit as recommended by the manufacturer (Qiagen, Hilden, Germany).

TRANSFECTION OF YEAST CELLS

A modified protocol of Neukamm et al. [2002] was used for yeast transfection. Briefly, *S. cerevisiae* precultures were inoculated from 3- to 4-day-old cultures on YE plates (from −70°C glycerol stocks) and grown on YPD for 72 h. In the main culture, the cells were grown overnight to a cell density of 5–9 × 10^7 cells per ml in YPD. For each sample, 1 × 10^9 cells were harvested by centrifugation at 3,500*g*. Cells were washed twice in 17 ml sterile distilled water for 30 min each to make the cells competent for transfection by swelling. Then cells were resuspended in 1 ml of 1 M sucrose (pH 4) to a cell density of 1 × 10^9 cells ml^{-1}. Eight to fifteen microlitres of plasmid DNA (in distilled water) was added to the cells to a final concentration of 15 μg ml^{-1}, and the sample was mixed immediately at 300 rpm for a few seconds. Cells were harvested after 22 h of incubation at 28°C without agitation. Tubes were not hermetically sealed to avoid pressure formation during incubation. After harvesting the cells, 850 μl of the supernatant was discarded. Cells were exposed to a hypotonic shift by adding 450 μl of sterile distilled water in 150 μl of remaining sucrose solution. After this, three aliquots of 200 μl were spread on selective medium. After appropriate dilution, cells of each sample were spread on non-selective medium in duplicate to calculate the transfection rate as transfectants per surviving cell. Transfection rates of the deletion mutants in the figures presented in this article were divided by the transfection rate of the wild-type strain, resulting in a factor.

QUINACRINE 2HCL STAINING

Quinacrine staining was performed following a method modified from Perzov et al. [2002]. Cultivation of the cells followed the procedure described for yeast transfection. When the cells reached a concentration of 5–9 × 10^7 cells per ml, cells were harvested as described for the transfection procedure. 3 × 10^7 cells were resuspended in 90 μl YPD buffered with 100 mM Hepes to pH 7.6. To simulate transfection conditions, additional samples were washed in distilled water as described for the transfection method and resuspended in 1 M sucrose. Cells in sucrose were incubated for 22 h at 28°C. After this, cells were harvested and resuspended in 90 μl of fresh 1 M sucrose, buffered with 100 mM Hepes to pH 7.6. Ten microlitres of quinacrine stock (Fluka, Buchs, CH) was added to cells both in buffered YPD and in buffered sucrose at a concentration of

200 μM. After incubating cells with quinacrine for 10 min at 30°C, cells were harvested and washed three times in 100 mM Hepes buffer (pH 7.6) containing 2% glucose. Cells were resuspended in 50 μl washing buffer and 10 μl of cell suspension was used for fluorescence and phase-contrast imaging using poly-L-lysine coated slides. Cover glasses were fixed using nail polish. Photos were taken with a Zeiss Axioskop (Jena, Germany) and a Olympus C4000 Zoom digital camera (Tokyo, Japan) using the biostep Argus X1 software, version 2.2.8 (Jahnsdorf, Germany). Identical manual settings were used for all samples, and pictures were taken immediately after exposure to UV-light to reduce bleaching effects.

LUCIFER YELLOW-CH ACCUMULATION

Lucifer Yellow CH (LY-CH) accumulation assay was performed as described earlier by Dulic et al. [1991] with the following modifications: cells were grown, harvested and prepared for staining as described for quinacrine staining. After this, cells were resuspended in 90 μl YE or 1 M sucrose. Ten microlitres of a 40 mg ml^{-1} Lucifer Yellow stock (Sigma–Aldrich, Steinheim, Germany) was added immediately. Cells were incubated for 22 h at 28°C, followed by washing three times in ice cold washing buffer (50 mM sodium succinate, 10 mM sodium azide, pH 5, supplemented with 1 M sucrose for cells in sucrose). Finally, the cells were resuspended in 50 μl washing buffer. Visualisation and documentation followed the procedure described for quinacrine staining.

FM4-64 STAINING

A procedure modified from Vida and Emr [1995] was used to visualise vacuolar and endosomal membranes. Briefly, cells were grown, harvested and prepared for staining as described for quinacrine staining. After this, cells were resuspended in 90 μl YE or 1 M sucrose. Ten microlitres of FM4-64 stock (FM4-64 = SynaptoRed C2, Sigma–Aldrich), diluted in YE or 1 M sucrose from a 16 mM stock in DMSO, was added immediately to a final concentration of 80 μM. Cells were incubated with the dye for 10 min at 30°C. Cells were harvested, resuspended in 100 μl fresh YE or 1 M sucrose and incubated for 22 h at 28°C. Finally, the cells were harvested and resuspended in 50 μl YE or 1 M sucrose. Visualisation and documentation followed the procedure described for quinacrine staining.

STATISTICAL ANALYSIS

The reliability of transfection data was analysed using Student's *t*-test. Significance was defined as $P < 0.05$.

RESULTS

INHIBITING ENDOCYTIC TRANSPORT

Transfection efficiency was measured in mutants *rcy1*, *vps21*, *vps45*, *vps27*, *vps4* and *vam6*. Lucifer Yellow (LY-CH) accumulation was followed to determine endocytosis efficiency, and FM4-64 staining was followed to determine membrane dynamics in these mutants under transfection conditions. Intraendosomal and vacuolar pH-conditions were determined by quinacrine staining.

Transfection was assayed using 2-μm plasmid, pFL1, selecting for *URA3* prototrophs, and transfection efficiency was calculated in relation to the strain BY4741 (wild-type strain). The mutant *rcy1*, where the F-box protein Rcy1p is deleted, is involved in endocytosis at early endosomes [Wiederkehr et al., 2000], exhibits reduced transfection efficiency in comparison to the wild-type (Table I). Figure 1 shows *rcy1* cells stained with the LY-CH and FM4-64, and quinacrine HCl. *rcy1* exhibits wild-type acidification of the vacuole and accumulates LY-CH in small compartments near the plasma membrane, predominantly near sites of polarised growth (Fig. 1). The vacuolar accumulation of LY-CH is reduced in comparison to the wild-type.

The mutants *VPS21* and *VPS45* which act in the same protein complex in protein sorting from the TGN to the PVC/MVB [Burd et al., 1997] exhibit a 10-fold enhanced transfection efficiency (Table I). The *P*-value of the transfection efficiency in mutant *vps21* is 0.1 in contrast to the *P*-value of mutant *vps45*, which is lower than 0.05. As both proteins are involved in the same protein complex in protein sorting, and transfection efficiencies of both mutants are in the same range, the transfection efficiency determined for mutant *vps21* is considered reliable too. Vacuoles of both mutants are not acidified while some small acidic compartments are detectable near the vacuole (Fig. 1). LY-CH accumulates in small non-vacuolar compartments also near the plasma membrane; these are present in higher numbers than in the wild-type. FM4-64 staining experiments reveal stronger membrane accumulation in *vps21* and *vps45* cells in comparison to the wild-type.

Mutants *vps27* and *vps4*, having a class E *vps* defect which results in an enlarged late endosome, do not exhibit transfection behaviour significantly different from the wild-type (Table I), reduced vacuolar acidification and large acidified structures near the vacuolar membrane (Fig. 1). They do not accumulate LY-CH or FM4-64 in the vacuole, indicating very strong transport inhibition between the class E compartment and the vacuole. Large compartments near the vacuole are seen in LY-CH or FM4-64 stainings (Fig. 1), presumably representing class E compartments [Piper et al., 1995; Babst et al., 1997; Bowers et al., 2004].

Mutant *vam6* which is deleted for a HOPS complex protein involved in vacuolar fusion and fusion of late endosomes to vacuolar membranes [Wada et al., 1992; Nakamura et al., 1997] exhibits a 15-fold enhanced transfection efficiency, and accumulates acidified vacuolar fragments. LY-CH and FM4-64 staining reveal some fragments with stronger dye accumulation, which are not near the plasma membrane. The *P*-value of the transfection efficiency of mutant *vam6* is higher than the significance threshold of 0.05 ($P = 0.15$). This variance may be due to the drastically altered phenotype of the mutant strain, which has a fragmented vacuole and is defect for fusion of late endosomal to vacuolar membranes. This multiple phenotype might lead to accumulation of endocytosed DNA and vacuolar proteins, involved in DNA degradation, sometimes in the same compartments and in other cases in different compartments. The distribution of endocytosed DNA between compartments with and without degrading enzymes can be variable which might explain the relatively high *P*-value of transfection efficiency data of *vam6*, even though a higher number of experiments were done with *vam6* in comparison to other mutants. We observed a positive effect of variable extent on transfection efficiency in every single experiment done.

TABLE I. Transfection Efficiencies of Endocytic Pathway Mutants

Mutant	t.e. (average)	s.d.	*P*-value (t.e.)	ρ	*P*-value (ρ)	Protein product	References
Wild-type	1.00	0.00	0.00	—	—	—	—
rcy1	0.30	0.14	0.06	1.00	0.00	Early endocytosis	Wiederkehr et al. [2000]
vps21	11.32	6.96	0.11	0.88	0.01	Import from TGN and early in late endosome	Gerrard et al. [2000], Horazdovsky et al. [1994]
vps45	10.73	6.78	0.02	0.71	0.07	Import from TGN in late endosome; in the same complex with Vps21p in this pathway	Burd et al. [1997]
vps27	2.24	2.44	0.07	1.00	0.00	Associated with ESCRTI subcomplex; required for proper sorting of ubiquitinated cargo in the MVB; export from the MVB	Piper et al. [1995], Bilodeau et al. [2003], Bowers et al. [2004]
vps4	1.04	0.49	0.07	1.00	0.00	Associated with ESCRTIII subcomplex; required for proper sorting of ubiquitinated cargo in the MVB; export from the MVB	Finken-Eigen et al. [1997], Bowers et al. [2004]
vam6	16.04	11.69	0.15	0.88	0.01	Part of the HOPS-complex; involved in vacuolar fusion; fusion of late endosomal derived membranes to the vacuole	Wada et al. [1992], Nakamura et al. [1997]

t.e., transfection efficiency (transfection $rate_{mutant}$/transfection $rate_{wild\text{-}type}$); s.d., standard deviation; *P*-value, probability that the null hypothesis explains the result observed; ρ, Spearman's rank correlation coefficient (here: correlation between transfection rates of mutant and wild-type).

While standard staining was done in YE medium, staining was additionally performed under transfection conditions in 1 M sucrose solution. Results were comparable, except that accumulation of the endocytic dyes (LY-CH and FM4-64) was enhanced in near plasma membrane compartments and, in some cases, in near vacuolar compartments.

ENDOCYTIC/VACUOLAR PH-CONDITIONS

Mutants deleted for *STV1* and *VPH1* were analysed to determine the influence of V-ATPase on transfection in correlation with its localisation. While Stv1p is present in the V0 subunit of the V-ATPase in endosomes and Golgi, Vph1p an isoform to Stv1p is present in the vacuole [Manolson et al., 1994; Perzov et al., 2002]. Both Stv1p and Vph1p are homologous to the human *ATP6V0A1* protein. Transfection efficiency in the *stv1* mutant is enhanced by a factor of 17, and by a factor of 11.5 in the *vph1* mutant (Table II). Quinacrine staining reveals a slightly higher pH-value in *stv1* in comparison to the wild-type (Fig. 2), and lack of vacuolar acidification in the *vph1* mutant. *vph1* and *stv1* cells show a reduced LY-CH accumulation. FM4-64 accumulates slightly higher in vacuolar membranes in *vph1*, and more efficiently in non-vacuolar membranes in *stv1*. These data reveal a positive correlation between the altered endosomal/vacuolar pH-value, a defect in endocytic/vacuolar transport, and enhanced transfection efficiency.

It seems that, an endosomal/vacuolar pH-value that is higher or lower in comparison to the wild-type pH-values of the endosomal/vacuolar system, shows positive correlation with transfection efficiency.

In a mutant deleted for *NHX1* encoding a member of the NHE family of Na^+/H^+ exchangers, transfection efficiency is enhanced by a factor of 5. The deletion mutants *vcx1* and *pmc1*, deleted for a vacuolar Ca^{2+}/H^+ antiporter (Vcx1p) and a vacuolar Ca^{2+} transporting ATPase (Pmc1p), respectively, which are both involved in vacuolar Ca^{2+} accumulation, show a wild-type transfection behaviour. Except for a very weak positive effect in *vcx1* and a very weak negative effect on endosomal/vacuolar acidification in *pmc1*, no differences between *nhx1* and the wild-type were observed in quinacrine staining, and no differences either were observed for *nhx1*, *vcx1*, and *pmc1* and the wild-type in LY-CH and FM4-64 staining (data not shown).

AUTOPHAGY AND ALP SORTING PATHWAY

As we have observed that acidification affects sorting and transfection, we aimed to understand in more detail which one of the intracellular protein sorting pathways tested influences transfection efficiency.

Absence of Vps13p involved in transport from endosomes to the TGN does not significantly affect transfection efficiency (Table III). A slight positive effect on transfection efficiency was observed in a mutant deleted for the gene encoding for the retromer complex protein Vps17p. Here transfection efficiency is enhanced by a factor of 2. The most prominent effect on transfection was found in mutant *apl5*. Apl5p is involved in the ALP sorting pathway which bypasses the late endosome and directs cargo directly from the TGN to the vacuole. Deletion of *APL5*, coding for a protein homologous to the human Ap3d1, results in a 16-fold increase in transfection efficiency.

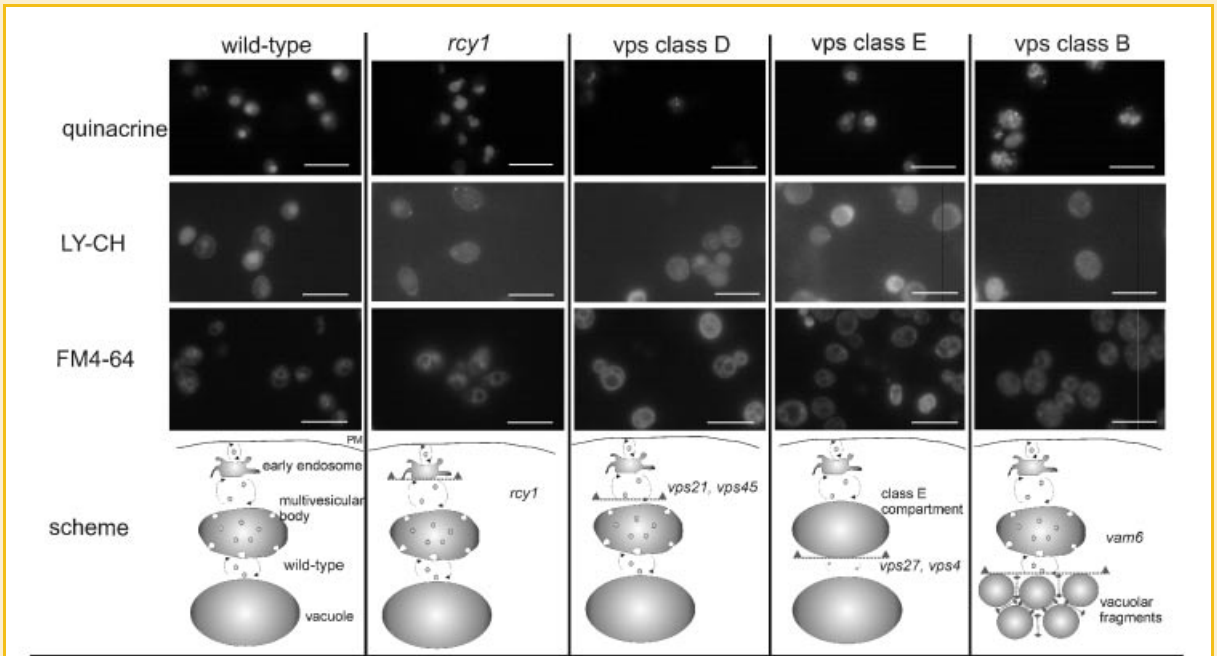

% of cells with a typical phenotype for

genetic background	wild-type cells	*rcy1* type cells	vps class D cells	vps class E cells	vps class B cells
wild-type	86.1	2.0	2.7	8.6	0.6
rcy1	8.4	86.2	2.8	2.1	0.5
vps21	3.9	5.3	85.1	3.5	2.2
vps45	1.1	3.0	91.1	3.3	1.5
vps27	3.5	2.9	8.7	83.7	1.2
vps4	0.7	2.3	15.2	79.8	2.0
vam6	0.0	0.0	1.5	1.4	97.1

Fig. 1. Impact of specific gene deletions of the endocytic pathway on vacuolar acidification, Lucifer Yellow (LY-CH) accumulation and membrane dynamics in BY4741 background in YE. Vacuolar acidification after 22 h was visualised using quinacrine-HCl staining. Quinacrine HCl accumulates in acidic compartments. Lucifer Yellow CH and FM4-64 were used to study endocytic uptake and membrane dynamics after 22 h. Photos of representative cells from one of at least three independent experiments were taken with FITC-fluorescence optics (quinacrine and LY-CH) or rhodamine optics (FM4-64) (upper panels), and with phase-contrast optics (lower panels). The bar represents 10 μm. Schematic illustration of the observations made is given below the pictures. Interrupting endocytic transport at different steps influences the transfection efficiency differently. The broken line with triangles represents the accumulation of endocytosed DNA. At the bottom the percentages of cells of the specific phenotypes in the samples tested are given. At least three independent experiments were done for each mutant.

In mutant *vac8*, transfection efficiency is enhanced by 8-fold, while deletion of *ATG19* did not have a measurable influence on transfection efficiency. This is also seen in deletion mutant *lap4*, encoding for API, which is sorted by Atg19p (data not shown).

Deleting the *PEP4* gene, which encodes the important vacuolar processing protease PrA, has a minor influence on transfection efficiency (two- to threefold increase).

Further yeast vacuolar processing and degrading proteases were assayed and did not prove relevant for transfection efficiency (data not shown).

Quinacrine, LY-CH and FM4-64 staining did not reveal significant changes in comparison to the wild-type for any deletion mutant described in this chapter.

DISCUSSION

Here yeast was used as a model to characterise endocytic transport and liberation of endocytosed DNA from endocytic/vacuolar compartments during DNA transfection. Further on, we studied the influence of endosomal/vacuolar pH-value, ion composition and hydrolase composition on transfection efficiency.

INFLUENCE OF ENDOCYTIC TRANSPORT AND HYDROLASE LOCALISATION

Non-viral transfection is based on the endocytic uptake, and thereafter endocytic transport of the vector construct. To elucidate the impact of inhibiting endocytic transport and protein sorting at different steps on transfection, we used endocytosis mutants (*rcy1*, *vps21*, *vps45*, *vps27*, *vps4* and *vam6*), Golgi to endosome/vacuole transport mutants (*vps13*, *vps17* and *apl5*) and CVT/autophagy mutants (*atg19* and *vac8*). Additionally, we analysed mutants of important yeast vacuolar processing proteases such as *pep4*. In particular, we were able to show a positive effect on non-viral transfection in *vps* class D mutants, as well as in mutant *vam6* and ALP-pathway mutant *apl5*.

TABLE II. Transfection Efficiencies of Ion Transport Mutants

Mutant	t.e. (average)	s.d.	*P*-value (t.e.)	ρ	*P*-value (ρ)	Protein product	References
Wild-type	1.00	0.00	0.00	—	—	—	—
stv1	16.84	2.31	0.01	1.00	0.00	Present in V0-subunit of V-ATPase at Golgi and endosomes	Perzov et al. [2002], Manolson et al. [1994]
vph1	11.62	3.47	0.01	1.00	0.00	Present in V0-subunit of V-ATPase at vacuole	Perzov et al. [2002], Manolson et al. [1994]
nhx1	6.77	4.17	0.05	0.80	0.16	$Na^+(K^+)/H^+$ antiporter at late endosome; ion homeostasis, intracellular pH and vesicle trafficking	Brett et al. [2005], Nass et al. [1997]
vcx1	0.55	0.11	0.00	1.00	0.00	Vacuolar Ca^{2+}/H^+ antiporter; vacuolar Ca^{2+} accumulation	Cunningham and Fink [1996], Miseta et al. [1999]
pmc1	1.02	0.20	0.01	1.00	0.00	Vacuolar Ca^{2+} transporting ATPase; vacuolar Ca^{2+} accumulation	Cunningham and Fink [1994, 1996]

t.e., transfection efficiency (transfection $rate_{mutant}$/transfection $rate_{wild\text{-}type}$); s.d., standard deviation; *P*-value, probability that the null hypothesis explains the result observed; ρ, Spearman's rank correlation coefficient (here: correlation between transfection rates of mutant and wild-type).

A negative effect on transfection efficiency we observed for mutant *rcy1*, which is involved in a very early step in endocytic transport; it can be assumed to be the result of less efficient liberation of DNA from these early endocytic compartments that accumulate endocytosed DNA during the transfection procedure (see Fig. 1).

In the mutant deleted for *VPS21*, endocytic transport is inhibited before DNA enters the PVC/MVB. This seems to reduce the contact of endocytosed DNA coming from the early endosome with degradation conditions and it results in enhanced transfection efficiency (Fig. 1). We assume that the enhanced transfection efficiency is due to the fact that many hydrolases, like PrA and others, are sorted via the CPY pathway from the TGN passing the PVC/MVB to the vacuole [Cooper and Stevens, 1996]. Contact of the endocytosed DNA to hydrolases using CVT/autophagy pathway and the ALP pathway is also avoided. The interpretation that reducing contact of endocytosed DNA to hydrolases is the reason for the observed positive effect on transfection efficiency is supported by analogous results for the *vps45* mutant. Vps45p and Vps21p both act in the same protein complex in transport processes from the Golgi to the endosomes [Burd et al., 1997]. Vps45p is involved in transport from the TGN to the PVC/MVB only, and not directly in endocytosis as Vps21p [Bryant et al., 1998]. We do not expect that Vps45p's impact on osmotic integrity affects the result of our transfection experiments [Yoshida et al., 1995], because we see comparable results for both *vps* class D mutants tested, *vps45* and *vps21*. Vps21p is not known to be involved in osmotic integrity.

Endosomal transport inhibition is also present in both the *vps45* mutant and *vps21* mutant. This might be due to sorting defects for proteins involved in further transport steps at the PVC/MVB. We did not observe these endosomal transport inhibitions in the mutant *vps17* which shows a significantly weaker positive effect on transfection efficiency.

Our data suggest that reducing the contact between hydrolases using the CPY pathway and endocytosed DNA enhances transfection efficiency. This effect is stronger when endocytic transport is inhibited before DNA enters the PVC/MVB.

Homotypic vacuolar fusion and fusion of vesicles or late endosomes with vacuolar fragments are inhibited in the *vam6* mutant which exhibits a fragmented vacuole and enhanced transfection efficiency [Wada et al., 1992; Nakamura et al., 1997] (Fig. 1). LY-CH and FM4-64 dyes were not accumulated in each compartment visible in phase contrast. Keeping in mind these significant transport defects, it might also be that in this mutant the compartments which accumulate endocytosed DNA probably do not contain hydrolases in the same distribution as in the wild-type vacuole. That would lead to reduced overall DNA degradation which might explain the enhanced transfection efficiency in *vam6*. It has earlier been described that there is a significant delay in processing of CPY and in accumulation of ALP [Nakamura et al., 1997] supporting this interpretation of the results of our transfection experiments. Furthermore, we were able to show that inhibiting the ALP pathway using *apl5* mutant results in enhancement of transfection efficiency as strong as in mutant *vam6*. An effect of the changed pH-value in the compartments accumulating endocytosed DNA cannot be excluded for mutant *vam6*, as non-equal

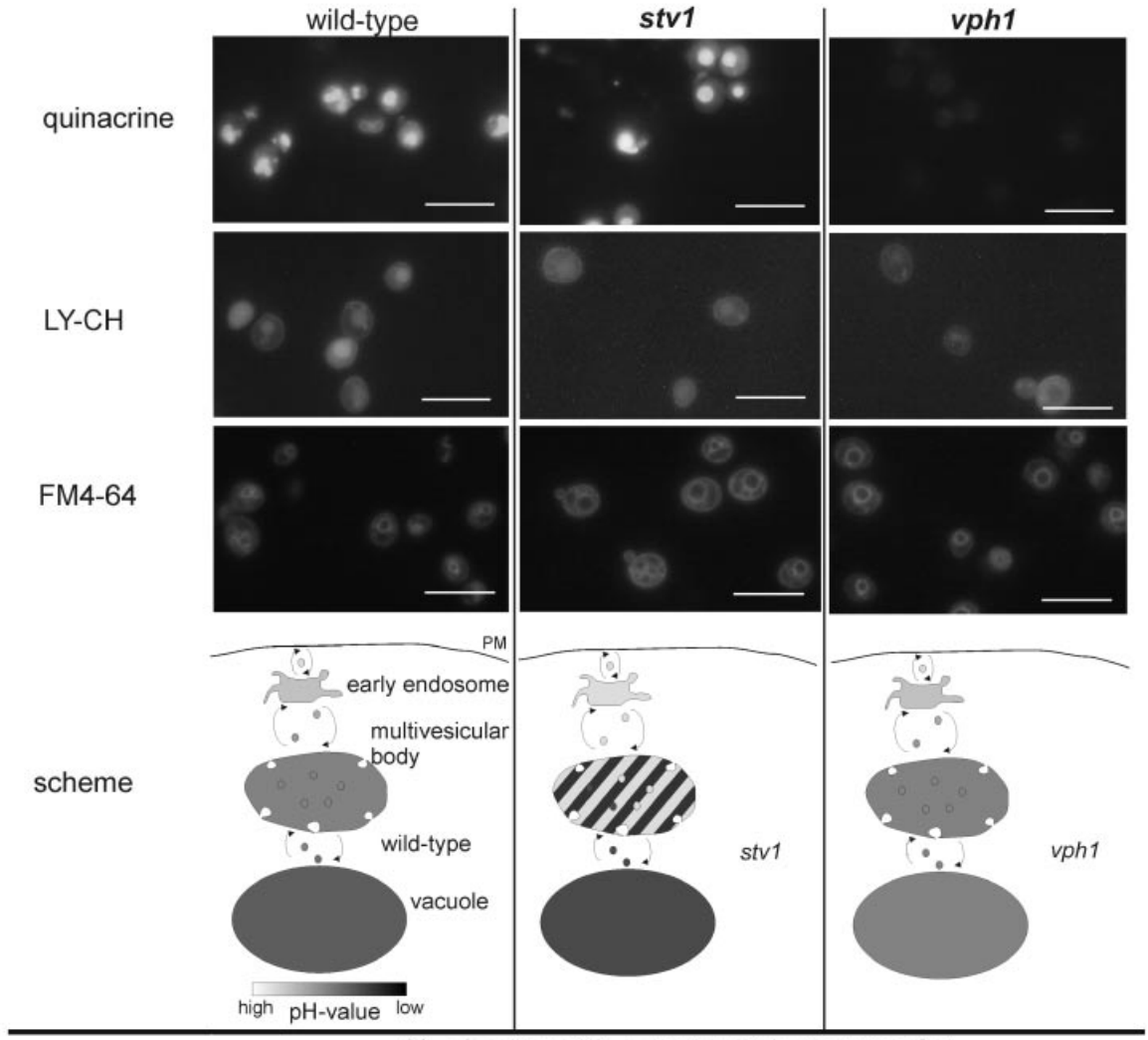

genetic background	% of cells with a typical phenotype for wild-type cells	*stv1* type cells	*vph1* type cells
wild-type	88.8	9.6	1.6
stv1	7.5	89.8	2.7
vph1	2.4	6.5	91.1

Fig. 2. Vacuolar acidification, endocytic uptake and membrane dynamics after 22 h in mutants deleted for *VPH1* or *STV1* in YE. See Figure 1 for experimental conditions. The bar represents 10 μm. Schematic illustration of the observations is given below the pictures. Non-wild-type endosomal/vacuolar acidification seems to be correlated to enhanced transfection efficiency. The acidification of the late endosomes in mutant BY4741 *stv1* remains unclear after quinacrine staining. At the bottom, percentages of cells of the specific phenotypes in the samples tested are given. At least three independent experiments were done for each mutant.

distribution of the V-ATPase in the compartments also has to be assumed.

These observations suggest that proteins which are involved in degradation and also maybe proteins which are involved in sorting endocytosed DNA are not only sorted via the CPY-pathway, but also via the ALP-pathway. Furthermore, the presence of a fragmented vacuole seems to be correlated to a enhanced liberation of non-degraded endocytosed DNA.

However, when a class E compartment is present such as in a *vps27* or *vps4* mutant, transfection efficiency is not significantly altered from that of the wild-type strain (Fig. 1). Both deletions tested lack a protein of the ESCRT complex [Bilodeau et al., 2003; Bowers et al., 2004]. Both are required for efficient sorting of ubiquitinated membrane proteins into the lumen of the MVB [Bilodeau et al., 2003; Bowers et al., 2004] and for export from the MVB to other organelles [Piper et al., 1995; Finken-Eigen et al.,

TABLE III. Transfection Efficiencies of Intracellular Transport Mutants

Mutant	t.e. (average)	s.d.	*P*-value (t.e.)	ρ	*P*-value (ρ)	Protein product	References
Wild-type	1.00	0.00	0.00	—	—	—	—
vps13	2.14	2.07	0.03	0.82	0.02	Seems to be involved in transport late endosome to TGN	Brickner and Fuller [1997]
vps17	2.11	0.53	0.02	1.00	0.00	Sorting nexin; part of the retromer complex; involved in CPY sorting	Köhrer and Emr [1993], Horazdovsky et al. [1997]
apl5	16.30	2.90	0.08	1.00	0.00	δ-adaptin like subunit of AP3 complex; clathrin-independent transport TGN to vacuole; ALP sorting	Panek et al. [1997], Darsow et al. [2001]
vac8	8.21	3.32	0.02	1.00	0.00	Involved in CVT/autophagy; involved in NVJ-dependent PMN; involved in homotypic vacuole fusion	Pan et al. [2000], Roberts et al. [2003], Wang et al. [1998]
atg19	0.73	0.23	0.01	0.40	0.58	Involved in CVT/autophagy (under N-starvation) of API (encoded by *LAP4*)	Scott et al. [2001], Shintani et al. [2002]
pep4	3.50	1.98	0.02	0.70	0.16	Important vacuolar processing protease; processes many other proteases and RNAses	Jones et al. [1982]

t.e., transfection efficiency (transfection $rate_{mutant}$/transfection $rate_{wild\text{-}type}$); s.d., standard deviation; *P*-value, probability that the null hypothesis explains the result observed; ρ, Spearman's rank correlation coefficient (here: correlation between transfection rates of mutant and wild-type).

1997]. Class E compartments accumulate plasma membrane, Golgi resident and endocytic markers as well as vacuolar proteins and exhibit quasi vacuolar conditions [Raymond et al., 1992; Piper et al., 1995; Rieder et al., 1996; Finken-Eigen et al., 1997]. These parameters result in near wild-type conditions for the endocytosed DNA and might explain the negligible effect of class E *vps* mutants on transfection efficiency.

Fluorescence staining shows that there is a strong transport inhibition from the class E compartment, and a vacuolar like acidification of these compartments.

These data indicate that vacuolar conditions and not the compartment per se in which the endocytosed DNA accumulates are responsible for near wild-type transfection efficiency. In addition to API, other hydrolases might enter the vacuole via the CVT/autophagy pathway [Scott et al., 2001]. Transfection efficiency is enhanced in the mutant deleted for *VAC8*, defect for a protein involved in autophagy. Autophagy resulting in the uptake of mitochondria into the vacuole is induced under nitrogen starvation conditions [Onodera and Ohsumi, 2005], as are present during the transfection incubation time of 22 h in sucrose. This might result in residual activity of, for example, the nuclear encoded mitochondrial nuclease Nuc1p in the vacuole before its degradation. In addition, DNases, involved in DNA repair mechanisms such as those from the RMX complex, might enter the vacuole via NVJ-mediated PMN, which is also induced by nutrient limitation conditions. Moreover, relaxation of supercoiled DNA as mediated by topoisomerases I–III might occur and play a role in degradation of endocytosed DNA. Any of this can be an explanation for the enhanced transfection efficiency of mutant *vac8*. CVT by Atg19p seems not to be relevant for transfection. Under starvation conditions, API bound to Atg19p in a CVT complex is transported to the vacuole via Atg19p-mediated binding to the preautophagosomal structure (PAS) followed by autophagocytosis [Shintani et al., 2002].

Finally, this suggests that degradation of endocytosed DNA is mediated by hydrolases sorted via CPY, ALP and autophagy pathways. Lytic protection and osmotic liberation of endocytosed DNA can be efficiently affected by inhibiting specific endocytic transport steps. To our knowledge, no homologues to human lysosomal DNases have been described in yeast until now to verify results described in the mammalian system previously in our yeast-based system.

PH-VALUE AND IONIC COMPOSITION OF THE ENDOCYTIC/VACUOLAR COMPARTMENTS

Endocytic/vacuolar membrane transport and protein sorting are regulated by the endo-compartimental pH-value [Klionsky et al., 1992; Brett et al., 2005]. Enzymatic activity and specificity is also influenced by ions, as in the case of Kex2p by K^+ ions [Rockwell and Fuller, 2002]. We could show that non-wild-type acidification of the endosomes and/or the vacuole is correlated to enhanced transfection efficiency, as demonstrated using deletion mutants *stv1* and *vph1* (summarised in Fig. 2). We were able to show a defect in transport caused by defects in endosomal/vacuolar acidification for transfection conditions. This correlation was described earlier by Klionsky et al. [1992] and Brett et al. [2005] for non-transfection conditions. Stv1p is present in the V-ATPase when it is located in the Golgi or

the endosomes [Manolson et al., 1994; Perzov et al., 2002]. The accumulation of membranes and the reduced LY-CH accumulation in the mutant deleted for *STV1* result from reduced membrane transport in earlier parts of endocytosis, a defect caused by altered pH in endosomes and Golgi. Not only the activity of proteins involved in endocytic transport is reduced under non-optimal pH conditions, but also sorting of proteins coming from the Golgi and located to endosomes and the vacuole is impaired. This, in consequence, leads to enhanced accumulation of endocytosed DNA in non-vacuolar compartments as, for example, in the *vps21* mutant which exhibits accumulation of membranes similar to *stv1* mutant (seen in FM4-64 staining). In addition, the transport of hydrolases into endosomes and vacuole and their activity is reduced, due to altered pH in these compartments. This in turn results in a positive effect on transfection efficiency, as endocytosed DNA has reduced contact with hydrolases in endosomes. This also applies to the *vph1* mutant, but here acidification and transport inhibition are stronger at the site of the vacuole, and weaker in early endocytosis in comparison to *stv1* mutant. This is due to the localisation of the protein deleted in the V0-subunit of the V-ATPase in the vacuole only [Manolson et al., 1994; Perzov et al., 2002]. This is seen as a slightly lower effect of *vph1* on transfection efficiency.

In mutants *vps21* and *vps45* which both show strongly enhanced transfection efficiency, we observe reduced vacuolar acidification. This is probably due to reduced V-ATPase levels, caused by the transport defect from the TGN to the PVC/MVB, and results in additional transport inhibitions in the endocytic pathway also in mutant *vps45*, which is known not to be involved directly in fusion of vesicles of the early endosome to the PVC/MVB [Bryant et al., 1998]. Due to this, altered endosomal/vacuolar pH-values are at least partly responsible for the positive effect on transfection efficiency in *vps21* and also *vps45* mutants.

Nhx1p is involved in the regulation of endosomal and cellular pH-value. A transport defect is observed in the *nhx1* mutant [Brett et al., 2005] and—maybe as a result of the effect on the pH-value—a positive effect on transfection efficiency is measured. The K^+-transport activity of Nhx1p might also affect enzymatic activity of endosomal/vacuolar hydrolases, as described for Kex2p [Rockwell and Fuller, 2002].

We deduce from these data that non-wild-type acidification of endosomal/vacuolar compartments slows down the transport of endocytosed DNA to the vacuole. We also hypothesise that mutants affected in acidification and endosomal potassium/sodium homeostasis exhibit higher transfection efficiency due to reduced degradation of endocytosed DNA.

Ca^{2+} accumulation in the vacuole does not seem to influence transfection, as deduced from unchanged transfection behaviour in mutants *vcx1* and *pmc1*. The transfection efficiency of mutants *vph1* and *vcx1* in comparison and the results of quinacrine staining in *vcx1* mutant (data not shown) indicate that the effect on vacuolar pH-value is negligible in mutant *vcx1* under transfection conditions.

The findings presented in this study are promising and will be used to optimise mammalian non-viral transfection in the future.

ACKNOWLEDGMENTS

We thank Roslin Bensmann for language corrections. Part of the study was supported by the BMBF in cooperation with RiNA GmbH and Cytonet GmbH & Co. KG.

REFERENCES

Akinc A, Langer R. 2002. Measuring the pH environment of DNA delivered using nonviral vectors: Implications for lysosomal trafficking. Biotechnol Bioeng 78:503–508.

Babst M, Sato TK, Banta LM, Emr SD. 1997. Endosomal transport function in yeast requires a novel AAA-type ATPase, Vps4p. EMBO J 16:1820–1831.

Baggett JJ, Wendland B. 2001. Clathrin function in yeast endocytosis. Traffic 2:297–302.

Bilodeau PS, Winistorfer SC, Kearney WR, Robertson AD, Piper RC. 2003. Vps27-Hse1 and ESCRT-I complexes cooperate to increase efficiency of sorting ubiquitinated proteins at the endosome. J Cell Biol 163:237–243.

Botstein D, Falco SC, Stewart SE, Brennan M, Scherer S, Stinchcomb DT, Struhl K, Davis RW. 1979. Sterile host yeasts (SHY): A eukaryotic system of biological containment for recombinant DNA experiments. Gene 8:17–24.

Bowers K, Lottridge J, Helliwell SB, Goldthwaite LM, Luzio JP, Stevens TH. 2004. Protein-protein interactions of ESCRT complexes in the yeast *Saccharomyces cerevisiae*. Traffic 5:194–210.

Brachmann CB, Davies A, Cost GJ, Caputo E, Li J, Hieter P, Boeke JD. 1998. Designer deletion strains derived from *Saccharomyces cerevisiae* S288C: A useful set of strains and plasmids for PCR-mediated gene disruption and other applications. Yeast 14:115–132.

Brett CL, Tukaye DN, Mukherjee S, Rao R. 2005. The yeast endosomal $Na^+(K^+)/H^+$ exchanger Nhx1 regulates cellular pH to control vesicle trafficking. Mol Biol Cell 16:1396–1405.

Brickner JH, Fuller RS. 1997. *SOI1* encodes a novel, conserved protein that promotes TGN-endosomal cycling of Kex2p and other membrane proteins by modulating the function of two TGN localization signals. J Cell Biol 139:23–36.

Bryant NJ, Piper RC, Gerrard SR, Stevens TH. 1998. Traffic into the prevacuolar/endosomal compartment of *Saccharomyces cerevisiae*: A *VPS45*-dependent intracellular route and a *VPS45*-independent, endocytic route. Eur J Cell Biol 76:43–52.

Burd CG, Peterson M, Cowles CR, Emr SD. 1997. A novel Sec18p/NSF-dependent complex required for Golgi-to-endosome transport in yeast. Mol Biol Cell 8:1089–1104.

Cooper AA, Stevens TH. 1996. Vps10p cycles between the late-Golgi and prevacuolar compartments in its function as the sorting receptor for multiple yeast vacuolar hydrolases. J Cell Biol 133:529–541.

Cunningham KW, Fink GR. 1994. Calcineurin-dependent growth control in *Saccharomyces cerevisiae* mutants lacking *PMC1*, a homolog of plasma membrane Ca^{2+} ATPases. J Cell Biol 124:351–363.

Cunningham KW, Fink GR. 1996. Calcineurin inhibits *VCX1*-dependent H^+/Ca^{2+} exchange and induces Ca^{2+} ATPases in *Saccharomyces cerevisiae*. Mol Cell Biol 16:2226–2237.

Darsow T, Katzmann DJ, Cowles CR, Emr SD. 2001. Vps41p function in the alkaline phosphatase pathway requires homo-oligomerization and interaction with AP-3 through two distinct domains. Mol Biol Cell 12:37–51.

Dulic V, Egerton M, Elguindi I, Raths S, Singer B, Riezman H. 1991. Yeast endocytosis assays. Methods Enzymol 194:697–710.

Finken-Eigen M, Röhricht RA, Köhrer K. 1997. The *VPS4* gene is involved in protein transport out of a yeast pre-vacuolar endosome-like compartment. Curr Genet 31:469–480.

Gerrard SR, Bryant NJ, Stevens TH. 2000. *VPS21* controls entry of endocytosed and biosynthetic proteins into the yeast prevacuolar compartment. Mol Biol Cell 11:613–626.

Horazdovsky BF, Busch GR, Emr SD. 1994. *VPS21* encodes a rab5-like GTP binding protein that is required for the sorting of yeast vacuolar proteins. EMBO J 13:1297–1309.

Horazdovsky BF, Davies BA, Seaman MN, McLaughlin SA, Yoon S, Emr SD. 1997. A sorting nexin-1 homologue, Vps5p, forms a complex with Vps17p and is required for recycling the vacuolar protein-sorting receptor. Mol Biol Cell 8:1529–1541.

Howell DP, Krieser RJ, Eastman A, Barry MA. 2003. Deoxyribonuclease II is a lysosomal barrier to transfection. Mol Ther 8:957–963.

Jones EW, Zubenko GS, Parker RR. 1982. *PEP4* gene function is required for expression of several vacuolar hydrolases in *Saccharomyces cerevisiae*. Genetics 102:665–677.

Kaksonen M, Toret CP, Drubin DG. 2005. A modular design for the clathrin- and actin-mediated endocytosis machinery. Cell 123:305–320.

Klionsky DJ, Nelson H, Nelson N. 1992. Compartment acidification is required for efficient sorting of proteins to the vacuole in *Saccharomyces cerevisiae*. J Biol Chem 267:3416–3422.

Köhrer K, Emr SD. 1993. The yeast *VPS17* gene encodes a membrane-associated protein required for the sorting of soluble vacuolar hydrolases. J Biol Chem 268:559–569.

Manolson MF, Wu B, Proteau D, Taillon BE, Roberts BT, Hoyt MA, Jones EW. 1994. *STV1* gene encodes functional homologue of 95 kDa yeast vacuolar H^+-ATPase subunit Vph1p. J Biol Chem 269:14064–14074.

Miseta A, Kellermayer R, Aiello DP, Fu L, Bedwell DM. 1999. The vacuolar Ca^{2+}/H^+ exchanger Vcx1p/Hum1p tightly controls cytosolic Ca^{2+} levels in *S. cerevisiae*. FEBS Lett 451:132–136.

Nakamura N, Hirata A, Ohsumi Y, Wada Y. 1997. Vam2/Vps41p and Vam6/Vps39p are components of a protein complex on the vacuolar membranes and involved in the vacuolar assembly in the yeast *Saccharomyces cerevisiae*. J Biol Chem 272:11344–11349.

Nass R, Cunningham KW, Rao R. 1997. Intracellular sequestration of sodium by a novel Na^+/H^+ exchanger in yeast is enhanced by mutations in the plasma membrane H^+-ATPase. Insights into mechanisms of sodium tolerance. J Biol Chem 272:26145–26152.

Neukamm B, Stahl U, Lang C. 2002. Endocytosis is involved in DNA uptake in yeast. Biochim Biophys Acta 1572:67–76.

Neukamm B, Weimann A, Wu S, Danevad M, Lang C, Geßner R. 2006. Novel two-stage screening procedure leads to the identification of a new class of transfection enhancers. J Gene Med 8:745–753.

Onodera J, Ohsumi Y. 2005. Autophagy is required for maintenance of amino acid levels and protein synthesis under nitrogen starvation. J Biol Chem 280: 31582–31586.

Pan X, Roberts P, Chen Y, Kvam E, Shulga N, Huang K, Lemmon S, Goldfarb DS. 2000. Nucleus-vacuole junctions in *Saccharomyces cerevisiae* are formed through the direct interaction of Vac8p with Nvj1p. Mol Biol Cell 11:2445–2457.

Panek HR, Stepp JD, Engle HM, Marks KM, Tan PK, Lemmon SK, Robinson LC. 1997. Suppressors of YCK-encoded yeast casein kinase 1 deficiency define the four subunits of a novel clathrin AP-like complex. EMBO J 16: 4194–4204.

Perzov N, Padler-Karavani V, Nelson H, Nelson N. 2002. Characterization of yeast V-ATPase mutants lacking Vph1p or Stv1p and the effect on endocytosis. J Exp Biol 205:1209–1219.

Piper RC, Cooper AA, Yang H, Stevens TH. 1995. *VPS27* controls vacuolar and endocytic traffic through a prevacuolar compartment in *Saccharomyces cerevisiae*. J Cell Biol 131:603–617.

Raymond CK, Howald-Stevenson I, Vater CA, Stevens TH. 1992. Morphological classification of the yeast vacuolar protein sorting mutants: Evidence for a prevacuolar compartment in class E vps mutants. Mol Biol Cell 3:1389–1402.

Rieder SE, Banta LM, Kohrer K, McCaffery JM, Emr SD. 1996. Multilamellar endosome-like compartment accumulates in the yeast *vps28* vacuolar protein sorting mutant. Mol Biol Cell 7:985–999.

Roberts P, Moshitch-Moshkovitz S, Kvam E, O'Toole E, Winey M, Goldfarb DS. 2003. Piecemeal microautophagy of nucleus in *Saccharomyces cerevisiae*. Mol Biol Cell 14:129–141.

Rockwell NC, Fuller RS. 2002. Specific modulation of Kex2/furin family proteases by potassium. J Biol Chem 277:17531–17537.

Scott SV, Guan J, Hutchins MU, Kim J, Klionsky DJ. 2001. *Cvt19* is a receptor for the cytoplasm-to-vacuole targeting pathway. Mol Cell 7:1131–1141.

Shaw JD, Cummings KB, Huyer G, Michaelis S, Wendland B. 2001. Yeast as a model system for studying endocytosis. Exp Cell Res 271:1–9.

Shintani T, Huang WP, Stromhaug PE, Klionsky DJ. 2002. Mechanism of cargo selection in the cytoplasm to vacuole targeting pathway. Dev Cell 3:825–837.

Vida TA, Emr SD. 1995. A new vital stain for visualizing vacuolar membrane dynamics and endocytosis in yeast. J Cell Biol 128:779–792.

Wada Y, Ohsumi Y, Anraku Y. 1992. Genes for directing vacuolar morphogenesis in *Saccharomyces cerevisiae*. I. Isolation and characterization of two classes of vam mutants. J Biol Chem 267:18665–18670.

Wang YX, Catlett NL, Weisman LS. 1998. Vac8p, a vacuolar protein with armadillo repeats, functions in both vacuole inheritance and protein targeting from the cytoplasm to vacuole. J Cell Biol 140:1063–1074.

Wiederkehr A, Avaro S, Prescianotto-Baschong C, Haguenauer-Tsapis R, Riezman H. 2000. The F-box protein Rcy1p is involved in endocytic membrane traffic and recycling out of an early endosome in *Saccharomyces cerevisiae*. J Cell Biol 149:397–410.

Wilber A, Lu M, Schneider MC. 2002. Deoxyribonuclease I-like III is an inducible macrophage barrier to liposomal transfection. Mol Ther 6:35–42.

Yarar D, Waterman-Storer CM, Schmid SL. 2005. A dynamic actin cytoskeleton functions at multiple stages of clathrin-mediated endocytosis. Mol Biol Cell 16:964–975.

Yoshida S, Ohya Y, Hirose R, Nakano A, Anraku Y. 1995. *STT10*, a novel class-D VPS yeast gene required for osmotic integrity related to the PKC1/STT1 protein kinase pathway. Gene 160:117–122.